Chemical Engineering Journal 466 (2023) 143051

Contents lists available at ScienceDirect

Chemical Engineering Journal

journal homepage: www.elsevier.com/locate/cej

Recyclable flame retardant phosphonated epoxy based thermosets enabled via a reactive approach

Wenyu Wu Klingler [a,*], Valentin Rougier [b], Zhenyu Huang [c], Dambarudhar Parida [a,d], Sandro Lehner [a], Andri Casutt [a], Daniel Rentsch [e], Karin Brändli Hedlund [f], Gion Andrea Barandun [f], Véronique Michaud [b], Sabyasachi Gaan [a,*]

[a] Laboratory for Advanced Fibers, Empa Swiss Federal Laboratories for Materials Science and Technology, Lerchenfeldstrasse 5, 9014 St. Gallen, Switzerland
[b] Laboratory for Processing of Advanced Composites (LPAC), Ecole Polytechnique Fédérale de Lausanne (EPFL), 1015 Lausanne, Switzerland
[c] Department of Polymeric Materials, School of Materials Science and Engineering, Tongji University, Shanghai 201804, PR China
[d] Sustainable Polymer Technologies (SPOT) TEAM, VITO NV, Boeretang 200, Mol, Belgium
[e] Laboratory for Functional Polymers, Empa Swiss Federal Laboratories for Materials Science and Technology, Überlandstrasse 129, 8600 Dübendorf, Switzerland
[f] Institute for Materials Technology and Plastics Processing, OST – Eastern Switzerland University of Applied Sciences, 8640 Rapperswil, Switzerland

ARTICLE INFO

Keywords:
Flame retardant epoxy thermoset
Phosphonate dynamic bonds
Reparability and reprocessability
Fire-safe coating
Flame retardant mechanism
Flax fiber reinforced composite

ABSTRACT

The development of reusable fire-safe polymers with a prolonged lifetime heralds the switch for a transition towards circular economy. In this framework, we report a novel phosphonated thermoset which is composed of networked phosphonate esters containing both P—C and P—O bonds. Employing a simple one-pot, two-step synthetic methodology, oxirane groups of the epoxy resin were partially reacted with various amounts of reactive bis H-phosphonate monomer, and cured with a cycloaliphatic hardener to obtain multifunctional thermosets with up to 8% phosphorus (P) content. Though 2.5% P was adequate to achieve good flame retardancy, a concentration > 5% P was necessary for accomplishing material reprocessability and recyclability. These phosphonated thermosets exhibited high T_g (94 °C – 140 °C) and good thermal stability. Fire performance of the thermoset with 2.5% P via cone calorimetry showed effective reduction in the peak heat release rate (pHRR, 75%) and significant inhibition of total smoke production (TSP, 72.5%), which was attributed to the gas and condense phase actions of the phosphonate moieties. This thermoset was explored as a transparent fire-safe coating on wood where an intumescent flame retardant mechanism was observed. The phosphonated thermoset with higher P content (6%) demonstrated excellent damage reparability and thermomechanical reprocessability driven by transesterification induced network rearrangement. This thermoset was used for manufacturing flax fiber reinforced composite, to demonstrate its future application as a polymer matrix for composite materials.

1. Introduction

Polymeric materials are ubiquitous and play an important role in almost all aspects of modern life. Due to their easy availability, versatility, and above all the unrivalled performance with low cost, they are indispensable in textile, packaging, transportation, and construction to consumer electronics applications [1,2]. In particular, the thermoset polymers that adopt a permanent shape after curing, are widely used in surface coatings, electronic encapsulation and advanced composite applications. Due to high density of covalent crosslinks in their network, they exhibit excellent chemical resistance, adhesive, electrical and mechanical properties [3]. The use of thermoset materials has increased in fire safety applications, including transportation, building and electronics [4]. Yet, the highly crosslinked covalent networks have intrinsic resistance to thermal reformation, and as a consequence they are not reprocessable nor recyclable [5,6].

From this standpoint, two major challenges in thermoset design have attracted growing attention in the scientific community: embedded fire safety and reprocessability/recyclability. To overcome the inherent flammable nature of polymer materials, reactive phosphorous-based flame retardants have been explored, and the resulting materials demonstrated increased fire safety and favorable environmental profiles

* Corresponding authors.
E-mail addresses: wenyu.wu@empa.ch (W. Wu Klingler), sabyasachi.gaan@empa.ch (S. Gaan).

https://doi.org/10.1016/j.cej.2023.143051
Received 1 February 2023; Received in revised form 27 March 2023; Accepted 16 April 2023
Available online 20 April 2023

with lower P concentrations as compared to materials containing non-reactive additives [7]. For example, the reactive P—H bond of DOPO allows direct covalent linkage to the epoxy network or to imine groups [8,9]. Nonreactive flame retardants are typically doped into the polymer matrix, which can cause environmental concerns owing to their leaching during usage or in landfills. Epoxy based thermosets containing phosphorus flame retardants are frequently employed in fire-safe applications. Currently such materials are landfilled or burned after use, leading to loss of valuable raw materials (i.e. phosphorus flame retardants) [10]. Earth's phosphorus is being depleted at a rapid rate and we will run out of it in few decades [11]. Thus, new solutions addressing these vital questions are the key to the development of new sustainable and safe materials.

The development of recyclable polymeric material with a prolonged useful lifetime will warrant a transition towards a more circular economy. By introducing dynamic crosslinks within the thermoset network, we can endow the networked material with self-healability, reprocessability or degradability by reversible exchange of the dynamic crosslinks, under certain external stimuli (such as heat, ultraviolet light, pH, etc.) [5,12]. Since Leibler's group reported the first "vitrimer" [13], materials with covalent adaptable networks (CANs) attained great attention in academic research and industry [14,15]. Different types of recyclable thermosets containing a wide variety of CANs have been reported [16,17], i.e. carboxylic ester [18], disulfide[19,20], siloxane [21], imine [22,23,24,25], diketoenamine [26], Diels – Alder adduct [27,28], dioxaborolane bonds [29] etc. The introduction of CANs ensures material integrity at working condition and allows stimuli-activated bond exchange above activation temperatures, thus rendering them recyclable.

Among the various CANs, phosphate/phosphonate ester linkages may provide a multifaceted solution to the above mentioned problems [30,31,32]. Normally recyclable and flame-retardant (FR) properties are introduced in a polymer matrix by multiple functional moieties, such as the combination of FR molecules with dynamic imine, ester or disulfide bonds [32,33]. In case of phosphate ester-based thermosets, the reprocessability based on transesterification [34] and fire protection brought by phosphorus, could be achieved simultaneously [35]. Phosphate chemistry are industrially relevant due to availability of raw materials which can be easily manipulated to develop reactive monomers. Therefore, studies of phosphate ester-based multifunctional vitrimer materials draw attention [36]. However, their practical use is still severely constrained by the relatively low thermal stability and poor hydrolytic stability. Theoretically, replacing the phosphate esters by phosphonates will bring more stable and non-hydrolysable P—C bonds. Thus it will improve the chemical stability of the resulting network and also increase the material's thermal stability [37], avoiding phosphorus unit leakage while maintaining the potential recyclability and flame retardancy.

To take advantage of the feasible chemistry of phosphorous esters, we in this work have designed and synthesized novel thermosets containing phosphonate networks via a one-pot and two-step process. In the first step, commercially available bisphenol A diglycidyl ether (DGEBA) resin was phosphonated partially by nucleophilic ring opening reaction with 2, 4, 8, 10-tetraoxa-3, 9-diphosphaspiro[5.5] undecane, 3, 9-dioxide (TDPSD), i.e. P—H bond to the oxirane ring. Subsequently an aliphatic curing agent was used to cure the modified resin. This procedure guaranteed solvent-free and controllable reaction conditions. The resulting P—C bonds in the phosphonated network ensure that the phosphorus moiety is fully integrated and won't leak into the environment during processing, use, and end-of-life treatment. By altering the molecular ratio of TDPSD and the amine hardener, thermosets with various P concentrations were synthesized. In addition to good flame retardancy, TDPSD inserted associative phosphonate ester bonds (P—O) into the cross-linked thermoset (EP-TDPSDs) matrix, which are in charge of material reprocessability and recyclability. We have systematically investigated the thermal properties, self-healing capability, reprocessability and flame retardancy of the EP-TDPSDs thermosets. The applications of these thermosets were explored, including their potential use in fire-safe coating and composite fabrication.

2. Experimental

2.1. Material

Pyridine, diphenylphosphite, triazabicyclodecene (TBD) and 1,8-Diazabicyclo[5.4.0]undec-7-ene (DBU) were purchased from Sigma-Aldrich (Switzerland) and used as received. All operations involving inert gas atmosphere or handling of air sensitive reagents and materials during synthesis were carried out using a Schlenk line. Bisphenol A resin (Epikote™ Resin 827) and isophorone diamine (IPDA, Epikure™ Curing Agent 943) were supplied by Hexion Specialty Chemicals GmbH, Germany. The flax fabrics purchased from Suter-Kunststoffe AG (Switzerland), were Bcomp's Amplitex 300 2/2 twill weaves.

2.2. Synthesis of 2,4,8,10-tetraoxa-3,9-diphosphaspiro[5.5]undecane 3,9-dioxide (TDPSD, bis spiroH-phosphonate)

The bis spiro H-phosphonate core **TDPSD** was synthesized via a transesterification/phosphonation approach reported earlier [38,39]. Typically, a double neck round bottle flask (100 mL) was charged with pentaerythritol (3 g, 22.03 mmol) and a magnetic stir bar. The flask was cooled down to 0 °C with an ice-bath, and connected to a dropping funnel with pyridine (30 mL) and diphenylphosphite (9.5 mL, 49.6 mmol). The mixture was slowly dropped to the pentaerythritol powder over a period of 20 min in a nitrogen atmosphere. The round bottom flask was removed from the ice bath and the mixture was stirred for 2 h at room temperature. Then 60 mL THF was injected into the flask via syringe, and the resulting suspension was vigorously stirred for 10 min to obtain white precipitates. The precipitate was filtered and washed twice with THF (10 mL each) and vacuum dried at 40 °C for 6 h with 65% yield **(TDPSD)**. The synthesis route (Figure S1) and detailed characterization are presented in the Supporting Information (Figure S2, Figure S3 and Table S1).

2.3. Preparation of phosphonated thermosets (EP-TDPSDs)

The detailed composition and acronyms of different thermosets synthesized in this work are summarized in Table 1. In a typical process, bisphenol A diglycidyl ether (DGEBA), a specific molar ratio of reactive bis spiro H-phosphonate (TDPSD) and appropriate amount of base (DBU) were thoroughly mixed and left at 80 °C for 2 h (Table 1). Subsequently, aliphatic amine hardener (IPDA), and for EP-TDPSD-5P/6P/8P, transesterification catalyst TBD, were added to the mixture at room temperature and mixed vigorously for 5 min. Subsequently, the mixture was poured into Teflon molds and cured. In order to cure the samples properly with or without the phosphonate units [40], a stepwise curing procedure at 100 °C for 2 h, another 2 h at 140 °C and a final curing (160 °C/2 h) was followed.

2.4. Flax fiber reinforced EP-TDPSD-6P composites

The flax plies were dried for 24 h at 80 °C after being cut, prior to fabricating the composites. The flax-TDPSD-6P composites were fabricated with 3 plies of pre-dried flax fabric and 3 g fine powder of ground EP-TDPSD-6P, resulting in composites with a fiber volume fraction $V_f \approx$ 40%. A hydraulic press was pre-heated at a temperature of 190 °C. Before pressing, a first layer of EP-TDPSD-6P vitrimer powder was spread at the bottom of a 72 × 45 mm^2 steel mold, and covered with a ply of flax fabric. This process was then repeated for all plies, with a final layer of polymer powder being deposited at the top of the stack before closing the mold. The mold was subsequently placed in the press and pressed for 20 min at a temperature of 190 °C with a pressure of 3.0 ±

Table 1
Formulation of the control sample and the TDPSD cured thermosets.

Thermosets	Bisphenol A resin (DGEBA, Epikote™ Resin 827)[a]	Isophorendiamine (IPDA, Epikure™ Curing Agent 943)	TDPSD	DBU	Triazabicyclodecene (TBD)	Measured P content (wt%)
EP-bl	1	0.5	0	0	/	0
EP-TDPSD-1.2P[b]	1	0.45	0.1	0.005	/	1.27
EP-TDPSD-2.5P	1	0.40	0.2	0.01	/	2.45
EP-TDPSD-4P	1	0.35	0.4	0.02	/	3.89
EP-TDPSD-5P	1	0.30	0.5	0.025	0.05	5.29
EP-TDPSD-6P	1	0.2	0.7	0.035	0.05	6.26
EP-TDPSD-8P	1	0.15	0.8	0.04	0.05	8.05

[a] all starting materials are in mol/mol ratio comparing to one equivalent of DGEBA.
[b] in EP-TDPSD-xP the numeric × indicates the measured weight content of phosphorus in percentage.

0.2 MPa, before demolding the composite.

2.5. Coating on wood (medium-density fibreboard)

Following the earlier mentioned thermoset preparation procedure, formulation EP-TDPSD-2.5P was used as thin coating on medium-density fibreboard (MDF). Initially, DGEBA (1 equivalent) was reacted with 0.2 equivalent of bis spiro H-phosphonate TDPSD (Table 1) at 80 °C for 2 h. Before applying the resin on MDF, 0.4 equivalent of aliphatic amine hardener (IPDA) was added to the mixture at room temperature and mixed vigorously for 5 min. Utilizing a thin film applicator (BGD 218, automatic film applicator, Guiged precise instrument), the resin mixture was applied homogenously on the surface of MDF with a paste gap of 1 mm. The coated MDFs were cured under 100 °C for 2 h, another 2 h at 140 °C and followed by final curing at 160 °C for 2 h. Finally, the coated MDFs were cut into 10 × 10 cm^2 test samples for further testing.

2.6. Characterization

^{1}H, ^{13}C and ^{31}P NMR spectra were recorded on a Bruker AV-III 400 spectrometer (Bruker BioSpin AG, Switzerland) using a 5 mm CryoProbe™ Prodigy probe at 400.2, 100.6 and 162.0 MHz, respectively. All NMR experiments were performed at 298 K using the Bruker standard pulse programs and parameter sets applying 90° pulse lengths of 12.0 μs (^{1}H), 10.5 μs (^{13}C) and 10.7 μs (^{31}P). ^{1}H and ^{13}C NMR chemical shifts (δ) were calibrated to residual solvent peaks and ^{31}P NMR chemical shifts were referenced to an external sample with neat H_3PO_4 at 0.0 ppm.

Solid-State NMR (ss NMR) measurements were performed on the same spectrometer employing a 4 mm CP MAS NMR probe. Approximately 50 mg of pulverized thermoset samples were filled into 4 mm zirconia MAS rotors. Spectra were recorded at 10 kHz sample rotation at room temperature applying the following parameters: 2.5 μs 90° excitation pulses on ^{1}H channel, 3 ms (^{13}C) and 2 ms (^{31}P) contact time (optimized for best signal to noise) with a ramp from 100 to 50% of power level on the proton channel, 3 s recycle delays, 100 kHz SPINAL 64 proton decoupling was applied during acquisition, and appropriate numbers of scans (^{13}C: up to 3072; ^{31}P: 256) were recorded to yield reasonable signal-to-noise ratios.

Phosphorus content of the composites was measured using the inductively coupled plasma optical emission spectrometry method (ICP-OES), on a 5110 ICP-OES (Agilent Switzerland AG, Basel, Switzerland) apparatus. Sample preparation for ICP-OES consisted of mixing 100 mg of a sample with 3 mL HNO_3, followed by digestion using a microwave.

ATR-FTIR spectra were recorded with a Bruker Tensor 27 FTIR spectrometer (Bruker Optics, Ettlingen, Germany), using a single reflection attenuated total reflectance (ATR) accessory with 4 cm^{-1} resolution, 32 scans and OPUS™ 7.2 software. In case of residues from fire tests, samples were collected from the burnt places and mixed properly prior to analysis.

Water resistance of the thermoset samples was carried out in 100% relative humidity according to ASTM D2247-15 standard. The chamber was pre-heated to 38 °C and maintained at 100% humidity. The samples were placed in the chamber for 24 h, and the sample weights before and after conditioning were recorded.

Thermogravimetric analysis (TGA) was performed on a NETZSCH TG 209 F1 instrument (NETZSCH-Gerätebau GmbH, Selb, Germany) under N_2 with a flow of 50 mL/minute. Temperature range from 25 to 800 °C at a ramp of 10 °C/minute was used for the analysis.

TGA-FTIR was used to analyze the gasses evolved during pyrolysis, using TGA instrument coupled with the Fourier-transform infrared spectrophotometer (Bruker Tensor 27). 10 mg of sample was heated from 25 to 800 °C at a rate of 10 °C/min^{-1}, and the FTIR spectra of the gases evolved during pyrolysis was recorded with a resolution of 4 cm^{-1} ranging from 4000 to 550 cm^{-1}.

Differential scanning calorimetry (DSC) were performed on the DSC 214 Polyma instrument (NETZSCH-Gerätebau GmbH, Selb, Germany) at a heating rate of 10 °C/minute (20 to 200 °C), under a N_2 flow (50 mL/minute) by running two repeating cycles. The glass transition temperature (T_g) was determined by using the "tangent method" as the meeting point of tangents to the curve, traced on the baseline and the peak side, on the low-temperature peak side.

UL 94 vertical burning tests of the thermosets flammability were assessed according to IEC 60695–11-10, with sample size of 13 × 125 × 3 mm^3.

Cone calorimetry (Fire Testing Technology, East Grinstead, London, UK) was performed with an irradiative heat flux of 50 kW/m^2 (ISO 5660 standard) on a specimen (100 × 100 × 3 mm^3) placed horizontally without any grid. Parameters such as heat release rate (HRR), peak of heat release rate (pHRR), average specific extinction area (SEA), total smoke release (TSR), total heat release (THR) and the final residue were recorded.

Heat release rate (HRR) was determined using pyrolysis combustion flow calorimeter (PCFC) (Fire Testing Technology Instrument, London, UK) following ASTM D7309. ~ 7 mg of the sample was exposed to a heating rate of 1.0 °C/s from 150 to 750 °C in the pyrolysis zone.

Direct inlet probe mass spectroscopic (DIP-MS) measurements were carried out using a Finnigan/Thermoquest GCQ ion trap mass spectrometer (Austin, TX, USA) equipped with a DIP module. **DIP-MS** was useful to detect possible volatile products. Nearly 1 mg of a composite sample taken in a quartz cup located at the tip of the probe was inserted into the ionization chamber. Measurements were performed at an ionization voltage of 70 eV, temperature of the ionic source of 200 °C, <10–6 mbar pressure and probe temperature ramp 60 °C/minute from 30 to 450 °C.

Scanning electron microscope (SEM) and Energy dispersive X-ray spectra (EDX) were recorded using a Hitachi S-4800 scanning electron microscope (Tokyo, Japan) equipped with Inca X-sight device from Oxford Instruments (Tokyo, Japan). During SEM measurements, acceleration was maintained at 2 kV and with emission current of 10 μA at a working distance of 8 mm. For EDX measurements, acceleration was

maintained at 20 kV and with emission current of 15 mA at a working distance of 15 mm.

Rheological tests were carried out on an Anton Paar Physica 301 MCR rotational rheometer (Austria). All tests were performed with a parallel plate fixture (plate diameter of 25 mm and gap of 1 mm). EP-TDPSD-6P powder was thermally processed into 1 mm plates using a hot press at 140 °C. The plates were then dried in a vacuum oven overnight at 80 °C prior to the measurements. Stress relaxation experiments were conducted after a 10 min temperature equilibration (140, 160, 180, or 200 °C respectively), a 5% strain step was applied and the stress was monitored over time. A constant normal force of 10 N was applied during all the measurements to ensure a good contact of the material with the parallel plates.

Dynamic mechanical analysis (DMA, model Q800, TA Instruments, Inc. New Castle, DE, USA) tests were carried out for evaluation of the mechanical performance changes before and after composite fabrication. A temperature sweep from 20 °C to 170 °C using multi-strain rate mode was performed, with a heating rate of 3 °C/minute at a frequency of 1 Hz, an amplitude of 10 μm and a force track of 125%. DMA test samples had a dimension around 60 mm × 12.5 mm × 1 0.4 mm.

Three-point bending tests were conducted according to ASTM-D790 standards. The measurements were performed using a Water + Bai Ag 125 kN universal testing machine, equipped with a 1 kN load cell, using displacement control at a velocity of 5 mm/minute. The crosshead position was recorded by the machine. The supports were made of steel rods which are free to rotate around their axis. The span length between the two lower supports was 51.5 mm. The measurements were performed at ambient conditions (25 ± 5 °C, 50 ± 10% RH). In a first stage, the crosshead was lowered until the upper rod came into contact with the specimen. This was determined through the detection of a small force (0.2 N for the blanks, 1 N for the composites). Once contact was made, the crosshead was moved down by 12 mm or until fracture, when applicable, and then positioned back to its initial position (1 mm above the position where contact was detected).

3. Results and discussion

3.1. Synthesis of phosphonated thermosets and their characterization

A one-pot and two-steps procedure was developed to prepare the multifunctional transparent epoxy thermosets with varied TDPSD contents (Fig. 1a). The chemical structure of the TDPSD was confirmed by 1D and 2D NMR spectroscopy (Figure S2 and S3). The flame retardant epoxy thermosets were analyzed by elemental analysis, ^{13}C and ^{31}P solid state NMR, and FTIR spectroscopy (Table 1, Figure S4, Fig. 1C, and Fig. 1d). A single ^{31}P NMR resonance at 6.5 ppm is observed for TDPSD in DMSO solution (Fig. 1b). In the solid state ^{31}P CP MAS NMR spectrum of the modified thermoset EP-TDPSD-4P, the resonance is shifted to 25.7 ppm (Fig. 1c) which is attributable to the formation of a P-CH_2 group instead of the originally present P—H bond. To further characterize the thermoset network, 13C CP MAS ss NMR spectroscopy was performed on EP-bl, EP-TDPSD-2.5P and EP-TDPSD-4P samples. The ^{13}C MAS NMR spectra of the three samples with broad and highly overlapping resonances are shown in Figure S4.

The above results demonstrated that the phosphonate P—C bonds were successfully introduced in the thermoset network. As well studies in the bioorganic community, the replacement of the bridging oxygen in a phosphate ester with a CH_2 could introduce stability and confer inertness to phosphatase cleavage [41]. In addition to the reprocessability of thermosets with phosphoester linkages (P—O) reported in the vitrimer field [36,31], the linkage of the phosphonate moiety via a non-hydrolyzable P—C bond eliminates potential leaching during use and recycling [42]. Molecular level distribution of phosphorus in the thermoset network can result in optimized fire performance at lower level of P loadings compared to a non-reactive approach [35,7,8,43].

The FTIR absorption peak around 2438 cm^{-1} attributed to the P—H bond in TDPSD, disappears in EP-TDPSD-2.5P and EP-TDPSD-4P

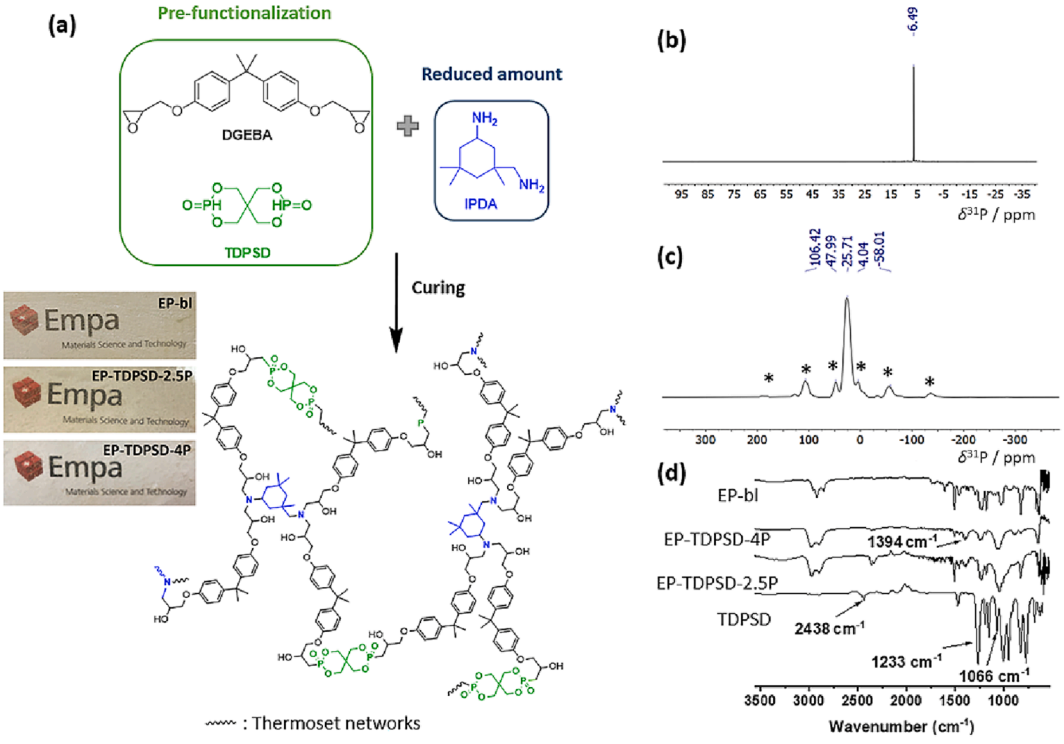

Fig. 1. (a) Synthesis procedure of reactive TDPSD cured epoxy based EP-TDPSDs thermosets, with optical pictures of the 1 mm thick plates on "Empa" envelope. (b) ^{31}P NMR spectrum of bis H-phosphonate TDPSD in DMSO-d_6 solution, (c) solid state ^{31}P CP MAS NMR of EP-TDPSD-4P (* = spinning side bands), and (d) FTIR spectra of the thermosets EP-bl, EP-TDPSD-2.5P, EP-TDPSD-4P and TDPSD.

(Fig. 1d). Importantly, the formation of the P—C bond is confirmed by the appearance of an absorption band at 1394 cm^{-1}, which is absent in TDPSD and EP-bl. They illustrate the full reaction of the TDPSD with the epoxy resin. The absorption peaks P—O—C appears at 1066 cm^{-1} for the modified thermoset. The peaks around 1607 cm^{-1}, 1510 cm^{-1} and 1225 cm^{-1} correspond to the aromatic ring of the epoxy structure and P═O of the TDPSD phosphorus moiety. Thus, it is clear that bis-H-phosphonate TDPSD was covalently incorporated in the epoxy matrix through the one pot, two steps synthesis method.

3.2. Fracture morphology of the novel thermoset

The SEM images of the fractured surfaces of EP-TDPSD-2.5P and EP-bl were investigated by scanning electron microscopy (Figure S5). The surface of fractured EP-bl displays regular cracks, which can be attributed to its relatively poor fracture resistance [44]. Whereas, EP-TDPSD-2.5P showed relatively homogeneous micro fracture morphology. Unavoidably, large scale bubbles are formed in the one pot, two steps co-curing procedure, fortunately without significant phase separation. The uniform fractured structure of EP-TDPSD-2.5P indicates the homogeneity of the TDPSD cured epoxy network without obvious aggregates [45].

3.3. Thermal properties

Highly cross-linked epoxy thermosets, have normally a softening temperature T_g (glass transition temperature), which determines its specific application range. T_g of thermosets are directly dependent on the state of its degree of cure and crosslink density [40]. After comparing the T_gs of EP-bl cured using the stepwise procedure (155.6 °C) and using a non-isothermal method (155.5 °C, Figure S6), we could confirm that the stepwise curing process could fully cure the systems we studied.

The origin of the softening via the glass transition is due to increased free volume of chains upon heating beyond T_g. Along with softening, the materials eventually show fluidity upon further heating. Conventional epoxy thermoset do not show fluidity upon heating because of its highly cross-linked network structure formed from stable bonds and restricted free chain motion [46]. As a consequence, fully cross-linked thermoset materials lose their recyclability due to the formation of a permanent network structure. However, the introduction of associative dynamic covalent P—O ester bonds in the thermoset can enable their potential recyclability without losing thermal stability [47,48]. Given the circumstances that sufficient ester bonds (P—O) already exist in the EP-TDPSDs epoxy thermoset, we predict that the epoxy network could repair via transesterification reaction under external stimuli when defects arise. Normally, the recycling temperature is located above the T_g and the initial decomposition temperature (T_{onset}). Therefore, we investigated the T_gs and T_{onset}s for determining the recycling temperature ranges at differant TDPSD loadings (Fig. 2a and 2c).

The T_gs of EP-TDPSDs were evaluated by DSC, which is generally ascribed to the segmental motion of the polymeric networks, and T_g is determined by the degree of freedom for the segmental motion, crosslinking and entanglement constraints, and the packing density of the segments [49]. As TDPSD is bifunctional, it tends to form linear macromolecules, inhibits crosslinking and as a consequence promotes segmental motion. Therefore all EP-TDPSD thermosets prepared in this work exhibited lower T_g than EP-bl (155 °C, Fig. 2c and Table 2) [6].

The thermal stabilities of the EP-TDPSDs with varying P contents were evaluated by TGA under N_2 atmosphere (Fig. 2) and relevant data are summarized in Table 2. The EP-TDPSD thermosets exhibited good

Table 2
Thermal analysis results obtained from DSC and TGA measurements for epoxy thermosets with increasing amount of TDPSD under nitrogen atmosphere.

Samples	T_g (°C)	T_{onset} [b] (°C)	T_{max} [c] (°C)	Residual yield at 800 °C (wt%)
EP-bl	155.6	351.7	369.5	5.8
EP-TDPSD-1.2P[a]	148.6	303.6	340.3	12.0
EP-TDPSD-2.5P	139.3	295.7	340.5	16.7
EP-TDPSD-4P	131.7	300.8	342.4	24.0
EP-TDPSD-5P	113.4	257.3	337.2	24.6
EP-TDPSD-6P	107.1	239.6	332.1	28.1
EP-TDPSD-8P	94.2	236.8	331.2	29.7

[a] Abbreviation of the bicyclic H-phosphonate co-cured epoxy resin. [b] Onset decomposition temperature, at which the thermoset undergoes 5 wt% weight loss. [c] Characteristic temperature, at which maximum rate of weight loss occurs.

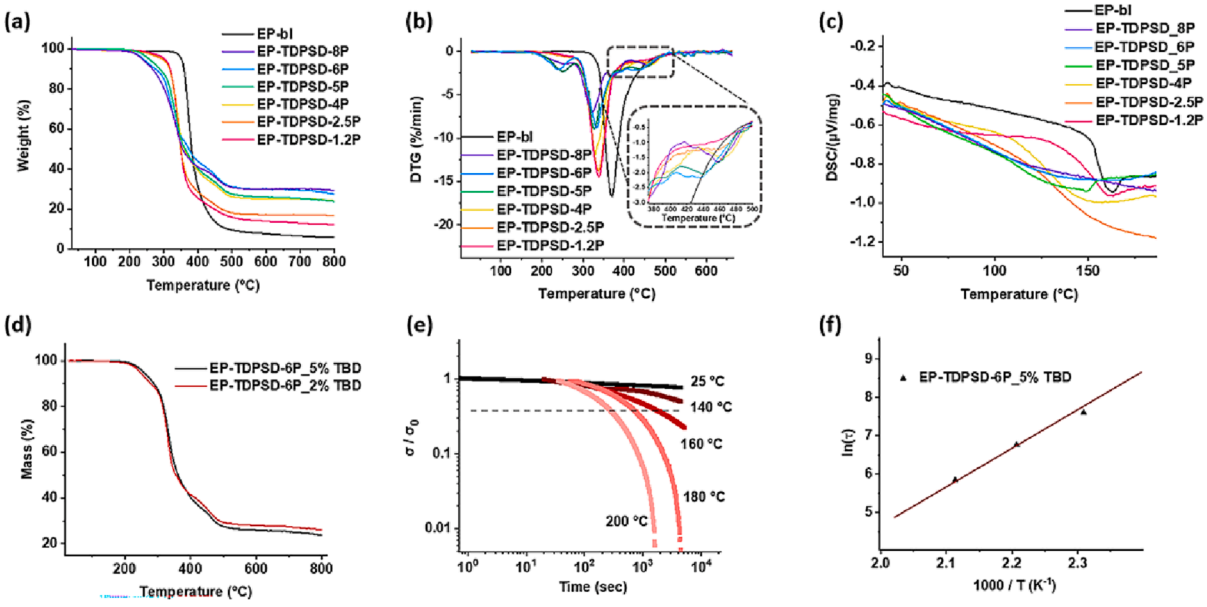

Fig. 2. (a) TGA and (b) DTG data of EP-bl and EP-TDPSD thermosets under nitrogen atmosphere, at a heating rate of 10 °C/minute, (c) DSC thermograms of the EP-TDPSDs, (d) TGA of EP-TDPSD-6P with varied amount of catalyst TBD, (e) stress relaxation curves of EP-TDPSD-6P at 10% strain under different temperatures up to 200 °C, where the stress (σ) is normalized by the initial stress (σ_0). The dotted line indicates the point at $\sigma/\sigma_0 = 1/e$ (=0.3679), and (f) fitting of the relaxation times τ to the Arrhenius plots as a function of inverse temperatures.

thermal stability, the temperatures of 5% mass loss (T_{onset}) for all samples are above 240 °C. Although T_{onset} decreases for the EP-TDPSD thermosets (Table 2), compared to 351.7 °C for EP-bl. EP-bl shows a one-step mass loss in the temperature range of 300–450 °C, while the EP-TDPSDs exhibit apparently-two or more thermal decomposition stages in the same range until 370 °C with an additional shoulder that extends over a range of approx. 100 °C as shown in the TGA and DTG curves (Fig. 2a and Fig. 2b). Additionally for EP-TDPSDs, a small decomposition step (approx. 9 wt%) appears at 455 °C. The data obtained above indicate the optimal reprocessing temperature, which lies between the glass transition temperature and the initial decomposition temperature (230 °C > T_{re} > 94 °C).

The transesterification catalyst, TBD, has negligible effect on the thermal stability of the EP-TDPSD thermosets (Fig. 2d). Even though the addition of TDSPC to the thermoset matrix catalyzes the decomposition to lower temperatures, a larger amount of char residue is formed at temperatures above 400C. In comparison of 5.8% char residue for EP-bl, EP-TDPSD-2.5P has almost three times the char residue (16.7%, Table 2), and EP-TDPSD-6P has significantly 5 times the char residue (28.1%). This indicates the potential condensation phase driven flame retardancy of EP-TDPSDs.

3.4. Recyclability and reparability

Considering sufficient associative dynamic phosphonate ester (P—O) bonds exist in the EP-TDPSD-5P/6P/8P, transesterification reaction can occur at elevated temperature above T_g as illustrated in Figure S7, Supporting Information. The transesterification induced dynamic bond exchange within the network is the driving force to obtain reprocessable thermosets, which can be monitored by rheological stress relaxation [48,50]. When they get heated up, the internal stresses can be released and thus the viscosity will be reduced [51]. Among the series of epoxy thermoset we designed, EP-TDPSD-6P revealed great stress-relaxation at high temperatures (>140 °C), meanwhile there was negligible stress-relaxation at room temperature. It follows a simple Arrhenius law with an activation energy of ~ 75 kJ/mol K as shown in Fig. 2f [52,53].

To demonstrate the healing capability of the phosphonate networked thermoset, the surface of EP-TDPSD-6P samples was sliced twice with a razor blade in a consequential way (Fig. S8a). When exposed to 160 °C in a pre-heated oven for 5 min, the scratches almost disappeared, and the damaged area became smoother. In addition, SEM analysis confirmed the microstructure reparability of the EP-TDPSD-6P. The surface was scratched multiple times with a point-tip tweezer to clearly reveal damaged area. The scratched epoxy surface appeared as a coarse, fractured and grainy ditch under SEM (Figure S9 a, c and e). After healing for one hour, the deep crack with grainy surface got smoother (Figure S9 b, d and f). To demonstrate the full healability of EP-TDPSD-6P when exposed to external mechanical damage (Fig. 3a), a strip of EP-TDPSD-6P was completely broken in two pieces (Fig. 3b). The broken pieces were put together and healed in a pre-heated oven under 160 °C for 5 min. The broken parts could rejoin without additional force or treatment (Fig. 3b), demonstrating its excellent healing capacity. Furthermore, after their repair using such mild and convenient conditions, the rejoined sample was able to withstand a weight of 200 g (Fig. S8b). The above observed macroscopic flow and reparability could reveal the intrinsic malleability and healability of the EP-TDPSD-6P, which is in the end mediated through the rearrangement of the thermoset network via phosphonate transesterification.

The thermomechanical recycling process is illustrated in Fig. 3c. In order to recycle the EP-TDPSD-6P bulk plate, it was ground into an opaque white powder via cryo ball-milling [54]. The cryo-grinded powder showed a particle size within 100 μm (Figure S10a). Then the fine powder is collected and evenly distributed in a rectangular-shaped metal mold. The set of samples were hot-pressed at 150 °C and 160 °C at a pressure of 6 MPa for 5 min. This process enabled that the powder fused into solid transparent plates again (Fig. 3c). The P—O ester bonds allow the dynamic exchange reaction, chain interpenetration and formation of new crosslinks. Under similar re-processing conditions the thermosets with higher P contents (more P—O bonds) could be easily pressed into homogenous plates again (Figure S10b), which is in

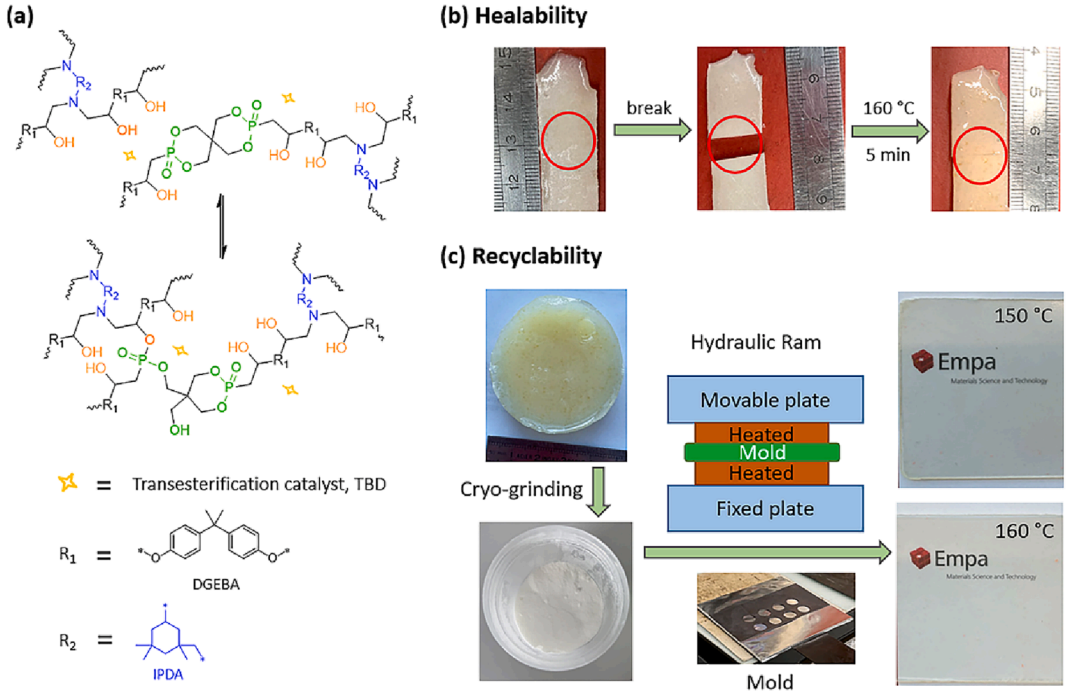

Fig. 3. (a) Schematic and chemical structure of the dynamic covalent network with the possible way of bond exchange; (b) Optical images of a piece EP-TDPSD-6P reconnected/healed at 160 °C for 5 min after being broken in the middle (red circle); (c) Thermal/mechanical recyclability demonstration of the cryo-grinded EP-TDPSD-6P fine powder using hydraulic hot pressing for 5 min at varied temperatures under a pressure of 6 MPa. (For interpretation of the references to colour in this figure legend, the reader is referred to the web version of this article.)

agreement with of the predicted transesterification mechanism. Recycling experiments of EP-TDPSD-4P and EP-TDPSD-5P were also performed. However, the lower the P contents (EP-TDPSD-5P and EP-TDPSD-4P), the higher the temperatures were required to obtain reprocessed sample plates. More specifically, it was enough to obtain transparent EP-TDPSD-6P plate at 140 °C for 5 min pressing time. Meanwhile, hot-pressing of EP-TDPSD-5P at 160 °C for 5 min resulted in an unfused particle-like appearance. Even higher treatment temperature (180 °C) and longer pressing time (20 min) were unable to generate uniform plates. No plate could be obtained for EP-TDPSD-4P, even after 20 min hot-pressing at 200 °C (Figure S10).

These results indicate that the reprocessability depends on the concentration of the phosphonate esters. As EP-TDPSD-6P was easy to fuse together under reasonable conditions in the hot press (Fig. 3c), it was considered an ideal candidate for further recycling and reprocessing experiments. This sample can be straightforwardly molded into desired shape by hot-pressing. The recycling of EP-TDPSD-6P can be repeated up to three times without dramatic mechanical, chemical and thermal property reduction (Figure S11). Only a slight decrease in the flexural strength (15%) and in thermal stability (T_{onset} from 239.6 °C to 230.4 °C), was observed after third recycling circle for this sample.

3.5. Flax fiber reinforced composites

From sport to automotive and aerospace industries, fiber reinforced polymer composites are widely used in various fields thanks to a combination of good mechanical properties and light weight [1,55]. Among them, epoxy based thermoset composites are often preferred or even irreplaceable when high performance is needed, which is the case in many applications like aircraft components and wind turbine blades. To demonstrate the potential use of the recyclable thermoset as a matrix, compression molding was carried out to fabricate flax fiber reinforced composites.

To achieve a good balance between reprocessing feasibility and satisfying thermal properties, EP-TDPSD-6P was chosen to demonstrate the application potential in fiber reinforced composites (Flax-TDPSD-6P). The EP-TDPSD-6P comprise sufficient covalent dynamic networks, which enable satisfying thermal stability, thermal malleability, and promising recyclability. It showed a relatively high T_g (107 °C) and T_{onset} (240 °C), and required reprocessing temperature lower than the degradation temperature of flax fiber. Yet, with the increase of covalent dynamic bonds the mechanical performance is reduced. This may be related to the lower molecular weight and the bi-functionality of the phosphorus units TDPSD [56]. EP-TDPSD-6P can be thermally activated to trigger bond exchange, allowing the network rearrangement without impairing their integrity. This means that composite processing by heating and pressing should enable the grinded powder to “soften” and impregnate the fibrous network. Thus, the fabrication of flax fiber reinforced thermoset composites was explored to obtain flame-retardant and recyclable materials. The composites were processed by compression molding, as presented in Fig. 4a. The composites were not fully impregnated due to the high viscosity of the matrix at the processing temperature, but nonetheless presented a good structural integrity.

Three point bending tests were conducted at room temperature on the resulting composites in order to access the effects of the fiber reinforcement on bending strength and modulus. Comparing to the thermoset matrix alone, the flexural strength increases more than 6 times from 8.7 MPa to 55.9 MPa for a fiber volume fraction of about 40%. The bending test curves and results are presented in Fig. 4b and Table S2, respectively. In addition, Young’s modulus (E) of the Flax-TDPSD-6P increased from 0.6 GPa to 9.4 GPa, compared to EP-TDPSD-6P. DMA temperature sweep exhibited a slight glass transition temperature change from 110.7 to 115.0 °C between the polymer matrix itself and the corresponding composite (Figure S12), which is consistent with the DSC measurement results (107.1 °C, Table 2). These preliminary tests demonstrated the feasibility of manufacturing flax fiber reinforced composite driven by the intrinsic malleability of the vitrimer-like materials.

3.6. Fire performance and potential application of the phosphonate thermosets

Considering the P nature in flame-retardant application, we forecast promising fire-safe application potential of the EP-TDPSDs thermosets [43]. From the TGA experiments, it was observed that the char residuals at 790 °C for EP-TDPSD-1.2P, EP-TDPSD-2.5P and EP-TDPSD-4P increased significantly to 12.0%, 16.7% and 24.0%, compared to a meagre 5.8% for EP-bl. This can be attributed to the addition of the reactive TDPSD which can promote the char formation and decrease the mass loss of epoxy during the main stage of thermal decomposition. In particular the pentaerythritol component of TDSP is known to be an excellent char former. The weight loss of the EP-TDPSD-6P at 370–470 °C is attributed to the further decomposition of char formed in the initial stage, which is consistent with the result of few earlier reports [57]. To gain further insight into the flame retardant mechanism of the thermosets which is relevant for determining suitable applications, detailed thermal analysis of EP-TDPSDs thermosets were performed.

Pyrolysis combustion flow calorimetry (PCFC) measurements were employed to evaluate the flammability of EP-TDPSDs thermosets on the micro- /bench-scale, and to gain information about the FR efficiency of the EP-TDPSDs (Figure S13a, Table S4). Compared to EP-bl (black curve), the peak heat release rate (pHRR) of EP-TDPSDs (colored curves) is reduced significantly, along with a simultaneous reduction in total heat release (THR) and temperature of peak heat release rate (T_m). The narrow HRR curves of EP-bl become broad for EP-TDPSDs, which indicates the flame inhibition of TDPSD via formation of thermally stable

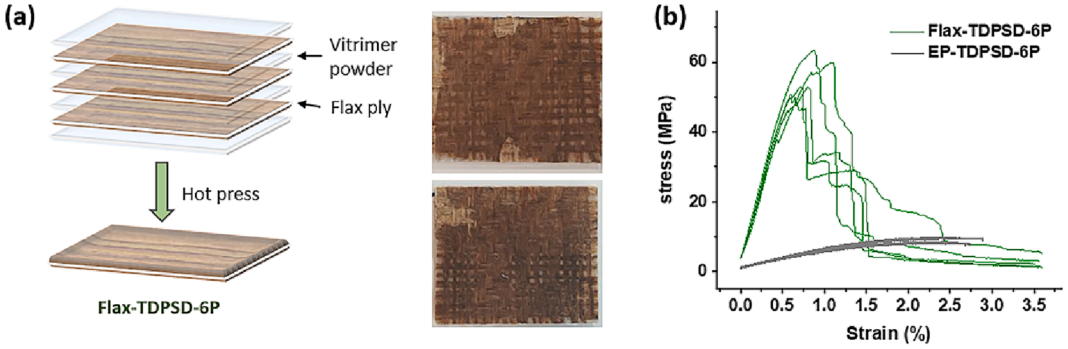

Fig. 4. (a) Schematic illustration of the flax fiber reinforced composite fabrication with two representative composite pictures, and (b) 3-point bending stress − strain curves of the EP-TDPSD-6P (grey curves) and Flax-TDPSD-6P composite with a polymer matrix volume fraction $V_m = 60\%$ (green curves). (For interpretation of the references to colour in this figure legend, the reader is referred to the web version of this article.)

char from the early stage of burning. This results in a slow heat release over a longer period of time for the EP-TDPSDs thermosets, unlike large amount of heat released in a short time in case of EP-bl.

Cone calorimeter tests (Figure S13b) showed that after ignition the heat release rate (pHRR) of EP-bl quickly increases to the peak value of 915 ± 20 kW/m^2 (pHRR). Whereas, pHRR values of EP-TDPSD-2.5P were only 230 ± 10 kW/m^2, which is reduced around 75%. The presence of TDPSD has also a strong influence in reducing the HRC (the maximum rate of heat release divided by the heating rate) by 36%, 42%, and 48% for EP-TDPSD-1.2P, EP-TDPSD-2.5P and EP-TDPSD-4P thermosets, respectively. The total heat release (THR) reduced from 120.4 MJ/m^2 to 31.6 MJ/m^2 (Figure S13c). In terms of the total smoke production (TSP), EP-TDPSD-2.5P showed a more significant TSP reduction of 9.2 m^2 (Figure S13d) than that of EP-bl (33.5 m^2), including CO_2 and NO gas reduction (Figure S13e and f). Significantly decrease of the TSP (72.5%), and effective inhibition of the peak heat release rate (57.3%) were noted.

The epoxy thermosets with and without reactive spirocyclic phosphonate TDPSD were subjected to a vertical flame spread test (UL 94) to assess their flammability. The results of the flammability tests are summarized in Table S4 and the digital photos of the UL94 tests and residues left after the fire tests are presented in Figure S14 and the supplementary videos. Epoxy thermoset with 2.5% of P content (EP-TDPSD-2.5P) achieved a UL 94-V0 classification (Figure S14). The right concentration of TDPSD in the epoxy thermosets matrix is crucial for achieving UL 94-V0 classification, as EP-TDPSD-1.2P containing only 1.2 wt% P burns partially and does not achieve any classification. Continuous burning, dripping and cotton ignition are observed after first ignition of the EP-bl. In contrast, the flame of EP-TDPSD-2.5P extinguishes within 3 s after two ignitions. The UL94 vertical flammability test and limiting oxygen index (LOI) test not only allow the evaluation of the flammability of the obtained formulations, but also provide information regarding the fire retardant mechanism of the investigated FR additives in epoxy. The reduced smoke evolution and the intumescent char formed during the burning process could contribute to the fire extinction.

We have compared certain properties of our work, i.e. fire performance and recyclability of the materials, with other phosphate ester- or carboxylic ester-based recyclable FR thermosets. As shown in the radar chart Fig. 5, the material characteristics including P contents, thermal properties (T_{onset} and T_g), and FR properties (UL94 rating and HRR) were compared. Meanwhile, recycling relevant features including the activation energy (E_a), recycling/reprocessing temperature and duration are also presented in the chart. Compared to the reference materials, the thermoset matrix developed in this work could achieve the lowest HRR (230 kW/m^2) with a low P (2.5%) content. Furthermore, the material requires relatively low recycling/reprocessing temperature and duration (i.e. 160 °C and 5 min).

3.7. Coating application on medium-density fibreboard (MDF)

Conventional epoxy thermoset coating materials have excellent water resistance. However, the introduction of polar phosphonate ester groups will affect the water resistant property of the materials. A simplified water resistance test was carried out to evaluate the water absorbance of the phosphonated thermosets. As shown in Table S5, the higher the P content of the matrix, the more water it gains after the test. The coating material EP-TDPSD-2.5P showed only 0.7% water gain, which is much lower than other EP-TDPSDs. Thus EP-TDPSD-2.5P can be considered as a suitable coating material for an outdoor application.

The demonstrated exceptional fire-resistance make them a good candidate for inflammable material protection, especially in transportation and building industries [61,62]. Based on the excellent fire inhibition and char forming property in the small scale fire test discussed earlier, we applied 1 mm thickness EP-TDPSD-2.5P coating on the surface of MDF samples (Figure S15), and investigated their fire resistance and heat isolation properties, as demonstrated in Fig. 6.

After five minutes of continuous ignition with Bunsen burner (flame temperature>1100 °C), the EP-TDPSD-2.5P coated MDF plate did not catch fire on the wood matrix, with its backside temperature reaching a maximum value of 106 °C (Fig. 6b and d), while the MDF blank burned completely with backside temperature reaching almost 550 °C (Fig. 6a and c). Very intumescent char was formed during the continuous ignition. After removal of the intumescent char, the underlying MDF matrix was found to retain its integrity (Fig. 6e). It could be concluded that EP-TDPSDs has a future perspective on flame-retardant surface treatments, including the potential for industrial implementation of this material. As summarized in Table S6, the weight loss of the MDF blank is about 74%,

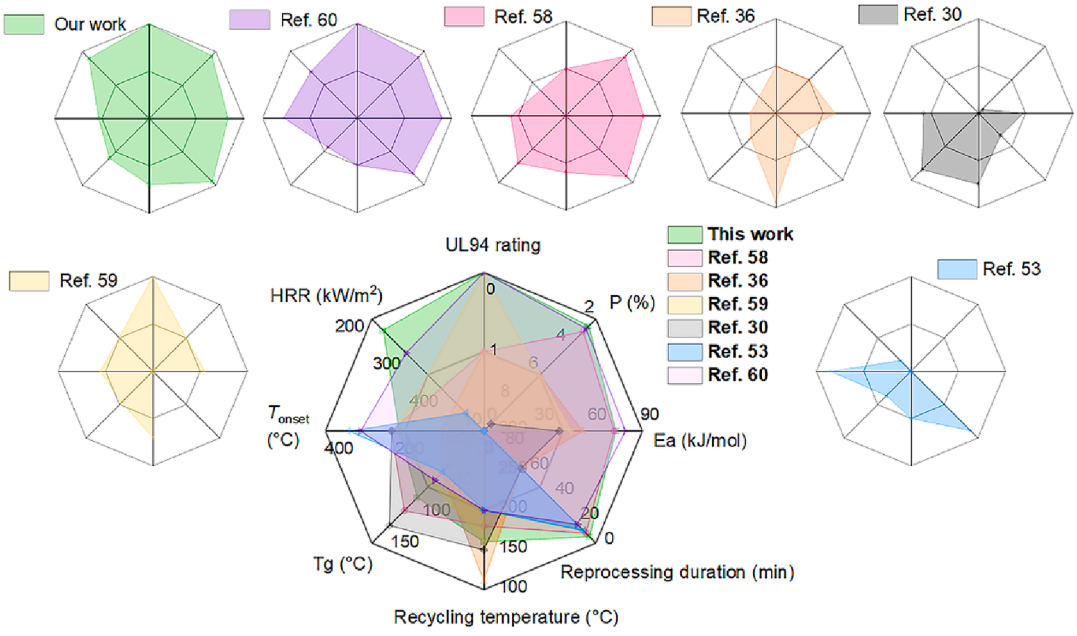

Fig. 5. Comparison of essential properties of reference materials (phosphate ester based thermosets [30,36,58,59], and carboxylic ester thermosets [53,60]) with the current work. The property is not reported when the number falls at middle point.

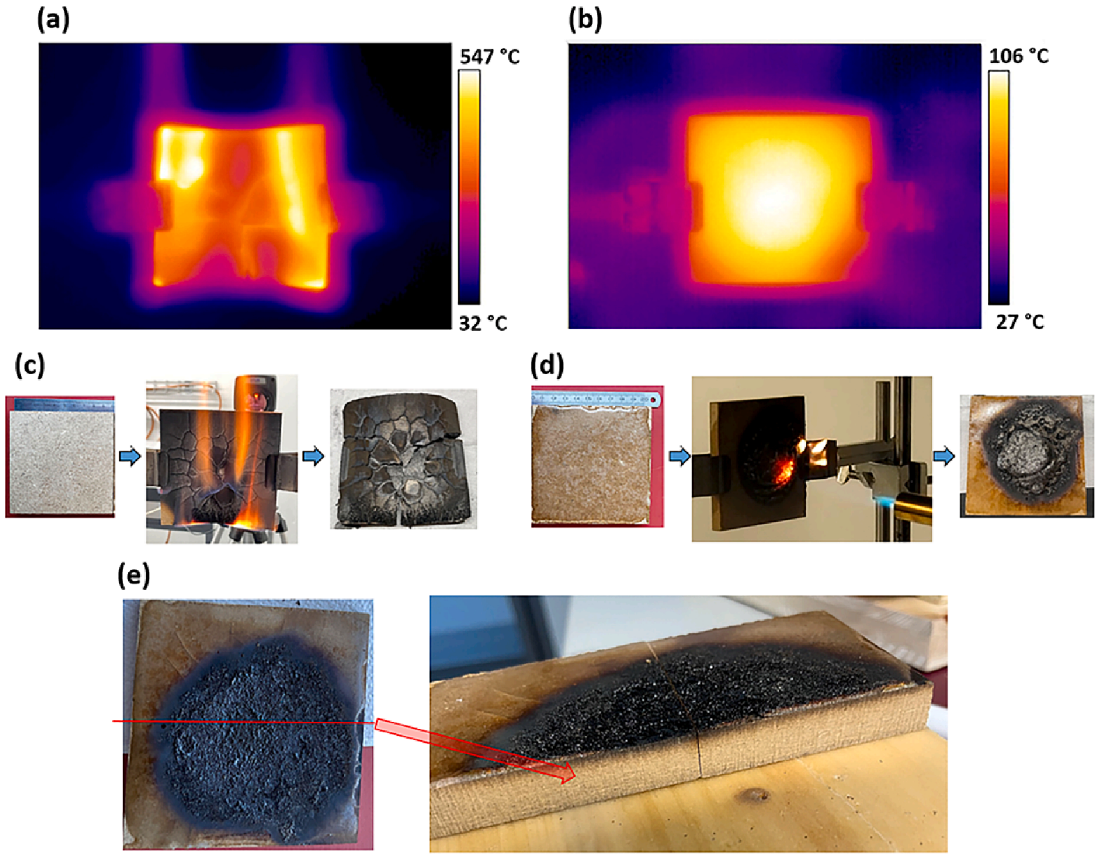

Fig. 6. (a) blank MDF samples and (b) EP-TDPSD-2.5P coated MDF sample were measured with 5 min continuous ignition using Bunsen burner (butane gas), with the maximal back temperature of the wood plate measured by IR camera, optical images of (c) the untreated and (d) the coated MDF samples after 5 min ignition, (e) surface and (e) cross section of the EP-TDPSD-2.5P coated MDF plate after burning test. All samples were located with distance to the blue flame ~ 50 mm (flame temperature ~ 1100 °C). (For interpretation of the references to colour in this figure legend, the reader is referred to the web version of this article.)

in contrast, only 6.8% was observed for the EP-TDPSD-2.5P coated MDF plate.

3.8. Fire inhibition mechanism

The thermal decomposition mechanism of the composites were investigated in detail by means of TGA-IR and DIP-MS analyses. FTIR spectra of volatile products formed in TGA at different temperatures is presented in Fig. 7. It can be observed that EP-TDPSD-2.5P produces significantly less volatile products than EP-bl. The volatile products of EP-bl increase with temperature, while EP-TDPSD-2.5P produces the most volatile products at 340 °C (T_{mas}) and then decreases gradually after 400 °C.

At 350 °C the infrared absorption peaks at 885 cm^{-1} and 931 cm^{-1} representing light alkenes and 966 cm^{-1} representing NH_3 were observed for EP-bl. Significantly lower intensity of these peaks were observed for EP-TDPSD-2.5P. Instead new peaks at 746 cm^{-1} and 1056 cm^{-1} corresponding to P—O containing species were observed for this sample. Peaks around 1343 cm^{-1} attributing to P—C containing species were also observed. With increased temperature, the sharp peaks around 1510 cm^{-1} corresponding to aromatics and aliphatic volatile components (3000–2840 cm^{-1}) in EP-bl are significantly suppressed for EP-PTODP-2.5P. In contrast carbonyl peaks (1790–1680 cm^{-1}) observed for EP-bl generally disappeared for EP-TDPSD-2.5P after 400 °C.

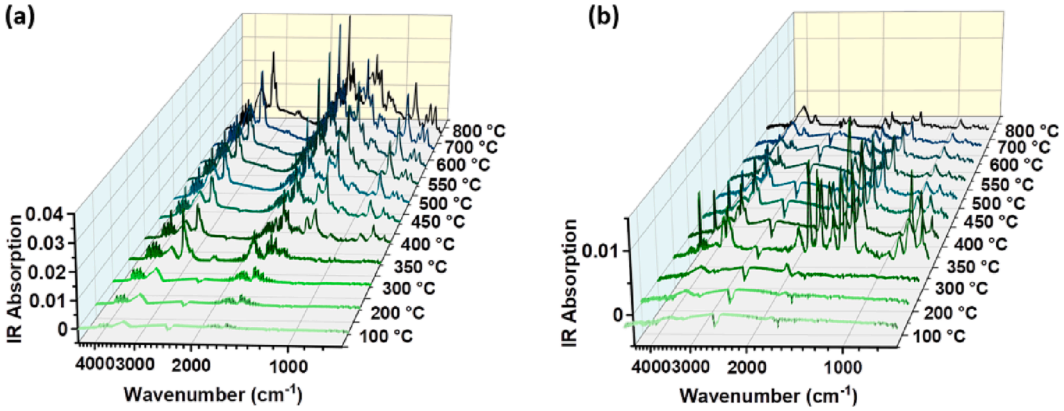

Fig. 7. TGA-FTIR spectra of the pyrolysis products from 10 mg of (a) EP-bl and (b) EP-TDPSD-2.5P at different temperatures.

Furthermore, all nitrogen containing volatile species (peaks at 1605 cm^{-1}, 1363 cm^{-1} and 775^{-1} assigned to N—O species, 1440^{-1}, 1458^{-1}, 2090^{-1} and 2246 cm^{-1} assigned to C—N containing highly toxic species) are minor or disappear for EP-TDPSD-2.5P. At the same time, for EP-TDPSD-2.5P peaks corresponding to H_2O are inconspicuous throughout the decomposition process (broad peaks around 3750–3500 cm^{-1} and 2000–1200 cm^{-1}).

Simultaneously, DIP-MS analysis indicates that the decomposition of the EP-TDPSD-2.5P produces a large amount of phosphorous species from 200 to 400 °C, whereas lower relative abundance of the volatile compounds were observed for the EP-bl (Figure S16). The formation of major fragments like PO radical (*m/z* 47) and 3-methyloxetane radical (*m/z* 71) initiates after 200 °C, while the HPO_2 radical (*m/z* 64) and other P-containing fragments evolve after 300 °C. The formation of these radicals confirm the strong flame inhibition action of TDPSD at an early stage. In air PO radicals can combine high energy H• and OH• species to form water [43], interrupting the combustion chain reaction which leads to flame inhibition. The above results of pyrolysis are consistent with the TGA-IR results to confirm a very effective gas-phase action of the phosphonate moieties.

3.9. Analysis of the char residue

It is widely recognized that phosphorus-based flame retardants play a very critical role in the condensed phase [61,63], and therefore, exploring the structure, morphology, and chemical composition of the char residue after the fire tests can contribute to the understanding of how TDPSD works. The surface morphology and elemental composition of EP-TDPSD-1.2P after combustion was characterized using scanning electron microscopy (SEM, Fig. 8) and energy dispersive X-ray spectrometry (EDS) mapping (Figure S17).

Compared to the compacted and fissured char residue of EP-bl (Fig. 8a, b and c), EP-TDPSD-2.5P left a distinct char with differences in the inner and outer layer. The residual outer layer (Fig. 8d, e and f) exhibited a coherent and sealed appearance, while the inner structure (Fig. 8g, h and j) was intumescent and porous. The closed outer layer could act as an effective physical barrier and lower gas flow. Besides, this porous char structure would prevent the heat transfer and the escape of volatiles. Therefore, we could anticipate that the inner layer is efficiently isolating heat and outer layer is blocking oxygen when EP-TDPSDs catch fire. EDX analysis showed a unified P distribution on the char residue (Figure S18), which also confirms that the covalent incorporation of TDPSD with epoxy was homogenous. These results together with the char yields in TGA experiments confirmed that the covalent incorporation of TDPSD phosphonate units in EP-TDPSDs play a major role in the formation of char during thermal degradation.

The chemistry of the char residues of EP-bl and EP-TDPSD-2.5P after fire tests were also characterized by FTIR (Figure S18). The broad absorption band at around 1592 cm^{-1}, 1486 cm^{-1}, and 1447 cm^{-1} represent C═C stretching vibration of polyaromatic carbons. This strong absorption band indicates that the incorporation of TDPSD into the epoxy thermoset enabled formation of sufficient aromatic component in the char. Peaks observed at 1202 cm^{-1} and 1168 cm^{-1} was attributed to P═O, at 1088 cm^{-1}, 992 cm^{-1} and 901 cm^{-1} of P—O vibration. The absorption peak appearing at 973 cm^{-1} was attributed to -P(=O)-O-. It indicates that the condensed phase of EP-TDPSDs contained significant residue rich in phosphorus.

These results demonstrated that the flame retardancy of TDPSD modified epoxy thermosets was not due to one single mechanism but rather a complex combination of mechanisms, including the gas phase mechanism and the condensed phase mechanism (Fig. 9) both caused by the covalent incorporated phosphonate units.

4. Conclusions and outlook

In this work we have developed novel phosphonated thermosets with

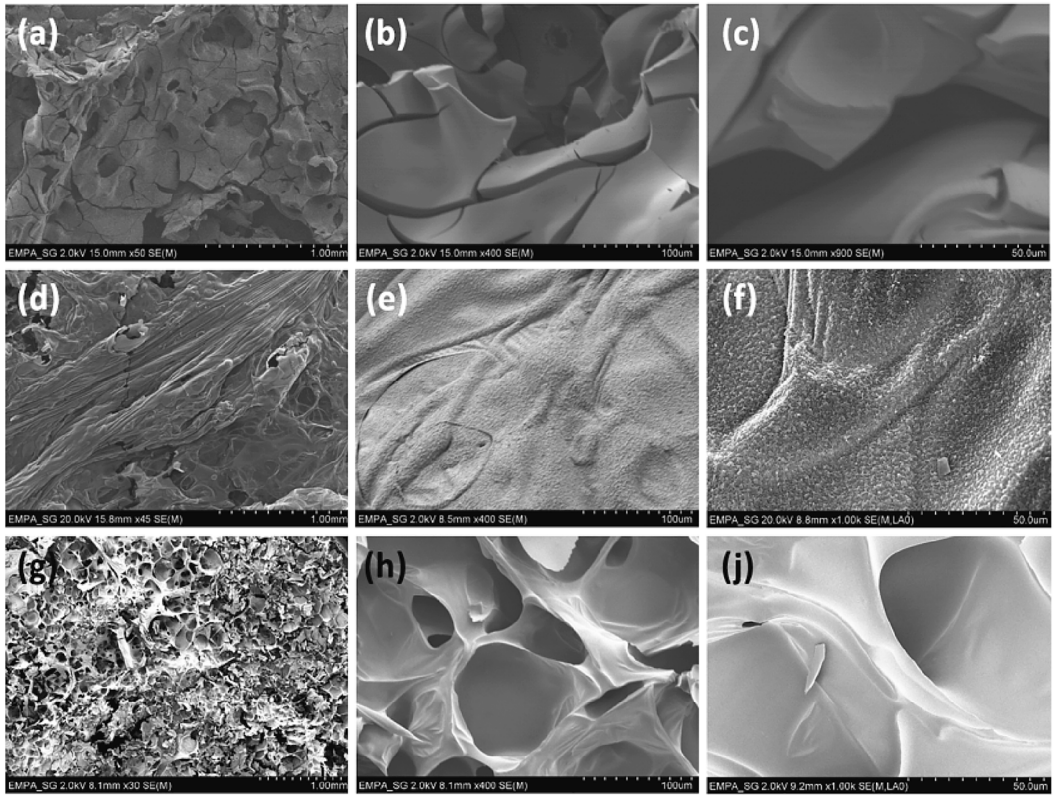

Fig. 8. SEM images of the residual chars for EP- bl outer surface (a, b, and c), flame-retardant thermosets EP-TDPSD-1.2P outer surface (d, e, and f), and EP-TDPSD-1.2P inner surface (g, h, and j) at difference magnification obtained from the UL-94 tests.

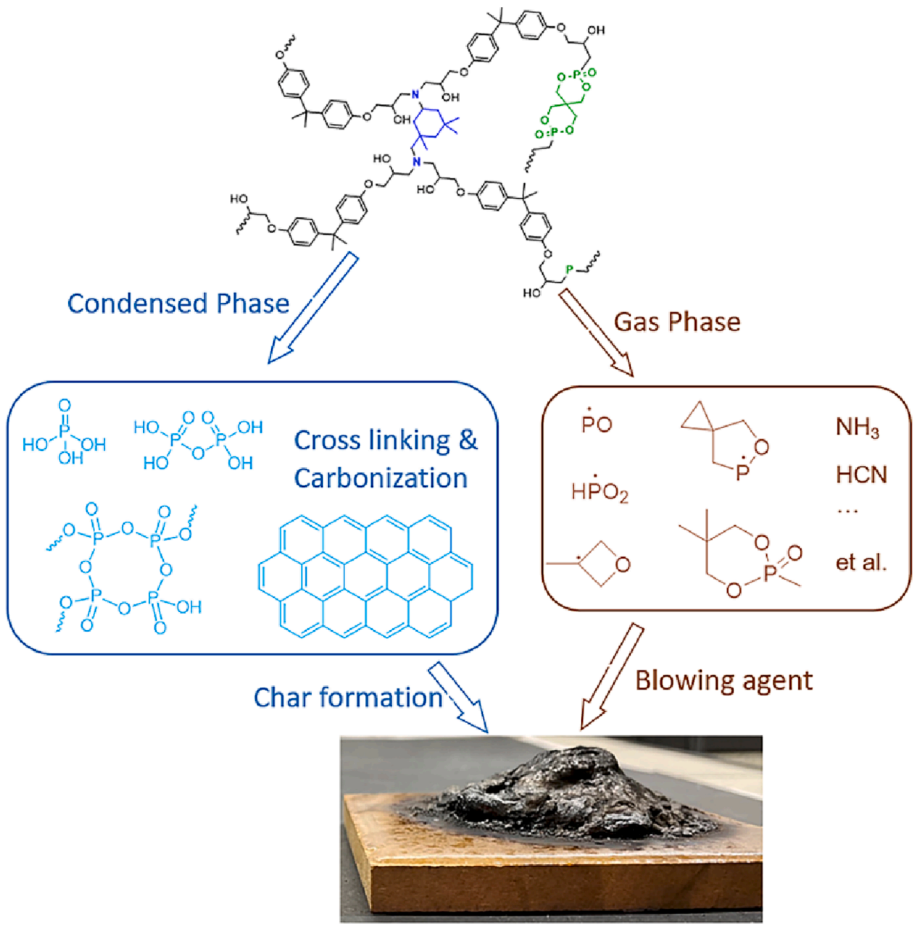

Fig. 9. Proposed decomposition mechanism of EP-TDPSDs (according to DIP-MS and TG-FTIR) via both gas phase and char forming actions.

inherent flame retardancy and good reprocessability and recyclability, which are introduced by the phosphonate moieties. A one-pot and two-step process, using varied ratios of DGEBA resin, reactive TDPSD and a cycloaliphatic hardener, has been evaluated to synthesize transparent multifunctional thermosets. The phosphonate ester CANs brought by the covalently networked TDPSD enable not only enhanced fire protection but also render the thermoset recyclable. A concentration of 2.5% P was adequate to achieve high flame retardancy, whereas 6% P was necessary for damage reparability after scratching, reprocessability and also recyclability.

For thermoset with 2.5% P, cone calorimetry investigations showed reduced peak heat release rate (up to 75%) during combustion and less smoke toxicity, which were attributed to the combination of gas and condensation phase actions of the phosphonate moieties. Flame retardant coating of this formulation on MDF exhibited excellent fire protection and heat isolation which was demonstrated by higher weight retention (93%) compared to the blank MDF (26%), owing to the outstanding intumescent nature of the char formed during fire test. The flame retardant polymer (EP-TDPSD-2.5P) has a potential in fire-safe transportation and electronic applications.

The reprocessability of the vitrimer-like EP-TDPSD-6P thermoset was investigated using thermomechanical recycling method. The presence of sufficient dynamic P—O ester bonds enabled transesterification based topological rearrangement during repairing and recycling, while retaining networked structure at room temperature. As an exploration for future application, flax fiber reinforced thermoset composites were fabricated via compression molding, which exhibited improved flexural strength (~6 time) compared to thermoset matrix. The utilization of these thermosets in fabricating fibers reinforced composites (such as carbon fiber, glass fiber, and natural fibers), as well as their chemical recyclability will be further examined in our future research. Our future work will also focus on the section of other phosphorus raw materials and adapting the manufacturing processes to improve the mechanical properties of these phosphonated thermosets.

The authors declare no conflict of interest. We confirm that this submission is original; it is not published elsewhere and is not under consideration for publication elsewhere.

Declaration of Competing Interest

The authors declare that they have no known competing financial interests or personal relationships that could have appeared to influence the work reported in this paper.

Data availability

Data will be made available on request.

Acknowledgments

We want to thank Ms. Milijana Jovic and Mr. Silas Keller from Additives and Chemistry group (Empa, St. Gallen, Switzerland) for their assistance during the cone calorimeter and pyrolysis flow combustion calorimetry tests, and Mr. Benno Wüst and Dr. Sithiprumnea Dul for their assistance in compression molding experiments of the blank thermosets. Dr. Wenyu Wu Klingler would like to acknowledge the support of the BNF Program, Bern University. We also thank the PhD exchange scholarship from China scholarship council (CSC) no. 202006260103 for supporting the stay of Mr. Zhenyu Huang at Empa. We further acknowledge Mrs. Hania Curjel for proof reading the manuscript and

English corrections.

Appendix A. Supplementary data

Supplementary data to this article can be found online at https://doi.org/10.1016/j.cej.2023.143051.

References

[1] A.K. Naskar, J.K. Keum, R.G. Boeman, Polymer matrix nanocomposites for automotive structural components, Nat. Nanotechnol. 11 (12) (2016) 1026–1030, https://doi.org/10.1038/nnano.2016.262.

[2] P. Song, H. Wang, High-Performance Polymeric Materials through Hydrogen-Bond Cross-Linking, Adv. Mater. 32 (18) (2020) 1901244, https://doi.org/10.1002/adma.201901244.

[3] A. Bifulco, D. Parida, K.A. Salmeia, R. Nazir, S. Lehner, R. Stämpfli, H. Markus, G. Malucelli, F. Branda, S. Gaan, Fire and mechanical properties of DGEBA-based epoxy resin cured with a cycloaliphatic hardener: Combined action of silica, melamine and DOPO-derivative, Mater. Des. 193 (2020), 108862, https://doi.org/10.1016/j.matdes.2020.108862.

[4] A.B. Morgan, The Future of Flame Retardant Polymers – Unmet Needs and Likely New Approaches, Polym. Rev. 59 (1) (2019) 25–54, https://doi.org/10.1080/15583724.2018.1454948.

[5] C.J. Kloxin, C.N. Bowman, Covalent adaptable networks: smart, reconfigurable and responsive network systems, Chem. Soc. Rev. 42 (17) (2013) 7161–7173, https://doi.org/10.1039/C3CS60046G.

[6] W. Post, A. Susa, R. Blaauw, K. Molenveld, R.J.I. Knoop, A Review on the Potential and Limitations of Recyclable Thermosets for Structural Applications, Polym. Rev. 60 (2) (2019) 359–388, https://doi.org/10.1080/15583724.2019.1673406.

[7] K.A. Salmeia, A. Gooneie, P. Simonetti, R. Nazir, J.P. Kaiser, A. Rippl, C. Hirsch, S. Lehner, P. Rupper, R. Hufenus, S. Gaan, Comprehensive study on flame retardant polyesters from phosphorus additives, Polym. Degrad. Stab. 155 (2018) 22–34, https://doi.org/10.1016/j.polymdegradstab.2018.07.006.

[8] G. You, Z. Cheng, Y. Tang, H. He, Functional Group Effect on Char Formation, Flame Retardancy and Mechanical Properties of Phosphonate–Triazine-based Compound as Flame Retardant in Epoxy Resin, Ind. Eng. Chem. Res. 54 (30) (2015) 7309–7319, https://doi.org/10.1021/acs.iecr.5b00315.

[9] X.-F. Liu, Y.-F. Xiao, X. Luo, B.-W. Liu, D.-M. Guo, L. Chen, Y.-Z. Wang, Flame-Retardant multifunctional epoxy resin with high performances, Chem. Eng. J. 427 (2022), 132031, https://doi.org/10.1016/j.cej.2021.132031.

[10] Y. Liu, Z. Yu, B. Wang, P. Li, J. Zhu, S. Ma, Closed-loop chemical recycling of thermosetting polymers and their applications: a review, Green Chem. 24 (15) (2022) 5691–5708.

[11] A.R. Jupp, S. Beijer, G.C. Narain, W. Schipper, J.C. Slootweg, Phosphorus recovery and recycling – closing the loop, Chem. Soc. Rev. 50 (1) (2021) 87–101, https://doi.org/10.1039/D0CS01150A.

[12] A. Adjaoud, L. Puchot, C.E. Federico, R. Das, P. Verge, Lignin-based benzoxazines: A tunable key-precursor for the design of hydrophobic coatings, fire resistant materials and catalyst-free vitrimers, Chem. Eng. J. 453 (2023), 139895, https://doi.org/10.1016/j.cej.2022.139895.

[13] D. Montarnal, M. Capelot, F. Tournilhac, L. Leibler, Silica-Like Malleable Materials from Permanent Organic Networks, Science 334 (6058) (2011) 965–968, https://doi.org/10.1126/science.1212648.

[14] J.D. Feist, D.C. Lee, Y. Xia, A versatile approach for the synthesis of degradable polymers via controlled ring-opening metathesis copolymerization, Nat. Chem. 14 (2021) 53–58, https://doi.org/10.1038/s41557-021-00810-2.

[15] N. Zheng, Y. Xu, Q. Zhao, T. Xie, Dynamic Covalent Polymer Networks: A Molecular Platform for Designing Functions beyond Chemical Recycling and Self-Healing, Chem. Rev. 121 (3) (2021) 1716–1745, https://doi.org/10.1021/acs.chemrev.0c00938.

[16] Z. Pei, Y. Yang, Q. Chen, E.M. Terentjev, Y. Wei, Y. Ji, Mouldable liquid-crystalline elastomer actuators with exchangeable covalent bonds, Nat. Mater. 13 (1) (2014) 36–41, https://doi.org/10.1038/nmat3812.

[17] J. Deng, X. Kuang, R. Liu, W. Ding, A.C. Wang, Y.C. Lai, K. Dong, Z. Wen, Y. Wang, L. Wang, H.J. Qi, T. Zhang, Z.L. Wang, Vitrimer Elastomer-Based Jigsaw Puzzle-Like Healable Triboelectric Nanogenerator for Self-Powered Wearable Electronics, Adv. Mater. 30 (14) (2018) e1705918.

[18] Y. Xu, S. Dai, L. Bi, J. Jiang, H. Zhang, Y. Chen, Catalyst-free self-healing bio-based vitrimer for a recyclable, reprocessable, and self-adhered carbon fiber reinforced composite, Chem. Eng. J. 429 (2022), 132518, https://doi.org/10.1016/j.cej.2021.132518.

[19] N. Tratnik, N.R. Tanguy, N. Yan, Recyclable, self-strengthening starch-based epoxy vitrimer facilitated by exchangeable disulfide bonds, Chem. Eng. J. 451 (2023), 138610, https://doi.org/10.1016/j.cej.2022.138610.

[20] H. Si, L. Zhou, Y. Wu, L. Song, M. Kang, X. Zhao, M. Chen, Rapidly reprocessable, degradable epoxy vitrimer and recyclable carbon fiber reinforced thermoset composites relied on high contents of exchangeable aromatic disulfide crosslinks, Compos. B Eng. 199 (2020), 108278, https://doi.org/10.1016/j.compositesb.2020.108278.

[21] X. Wu, X. Yang, R. Yu, X.-J. Zhao, Y. Zhang, W. Huang, A facile access to stiff epoxy vitrimers with excellent mechanical properties via siloxane equilibration, J. Mater. Chem. A 6 (22) (2018) 10184–10188, https://doi.org/10.1039/C8TA02102C.

[22] H. Liu, H. Zhang, H. Wang, X. Huang, G. Huang, J. Wu, Weldable, malleable and programmable epoxy vitrimers with high mechanical properties and water insensitivity, Chem. Eng. J. 368 (2019) 61–70, https://doi.org/10.1016/j.cej.2019.02.177.

[23] X. Zhang, Y. Eichen, Z. Miao, S. Zhang, Q. Cai, W. Liu, J. Zhao, Z. Wu, Novel Phosphazene-Based flame retardant polyimine vitrimers with Monomer-Recovery and high performances, Chem. Eng. J. 440 (2022), 135806, https://doi.org/10.1016/j.cej.2022.135806.

[24] W. Xie, S. Huang, S. Liu, J. Zhao, Imine-functionalized biomass-derived dynamic covalent thermosets enabled by heat-induced self-crosslinking and reversible structures, Chem. Eng. J. 404 (2021), 126598, https://doi.org/10.1016/j.cej.2020.126598.

[25] W. Xie, S. Huang, D. Tang, S. Liu, J. Zhao, Biomass-derived Schiff base compound enabled fire-safe epoxy thermoset with excellent mechanical properties and high glass transition temperature, Chem. Eng. J. 394 (2020), 123667, https://doi.org/10.1016/j.cej.2019.123667.

[26] P.R. Christensen, A.M. Scheuermann, K.E. Loeffler, B.A. Helms, Closed-loop recycling of plastics enabled by dynamic covalent diketoenamine bonds, Nat. Chem. 11 (5) (2019) 442–448, https://doi.org/10.1038/s41557-019-0249-2.

[27] L. Zhang, Z. Li, Q.-Q. Bi, L.-Y. Jiang, X.-D. Zhang, E. Tang, X.-M. Cao, H.-F. Li, J. Hobson, D.-Y. Wang, Strong yet tough epoxy with superior fire suppression enabled by bio-based phosphaphenanthrene towards in-situ formed Diels-Alder network, Compos. B Eng. 251 (2023), 110490, https://doi.org/10.1016/j.compositesb.2022.110490.

[28] X. Chen, A. Dam Matheus, K. Ono, A. Mal, H. Shen, R. Nutt Steven, K. Sheran, F. Wudl, A Thermally Re-mendable Cross-Linked Polymeric Material, Science 295 (5560) (2002) 1698–1702, https://doi.org/10.1126/science.1065879.

[29] M. Röttger, T. Domenech, R. van der Weegen, A. Breuillac, R. Nicolaÿ, L. Leibler, High-performance vitrimers from commodity thermoplastics through dioxaborolane metathesis, Science 356 (6333) (2017) 62–65, https://doi.org/10.1126/science.aah5281.

[30] X. Feng, G. Li, Versatile Phosphate Diester-Based Flame Retardant Vitrimers via Catalyst-Free Mixed Transesterification, ACS Appl. Mater. Interfaces 12 (51) (2020) 57486–57496, https://doi.org/10.1021/acsami.0c18852.

[31] S. Majumdar, H. Zhang, M. Soleimani, R.A.T.M. van Benthem, J.P.A. Heuts, R. P. Sijbesma, Phosphate Triester Dynamic Covalent Networks, ACS Macro Lett. 9 (12) (2020) 1753–1758, https://doi.org/10.1021/acsmacrolett.0c00636.

[32] W. Wu Klingler, A. Bifulco, C. Polisi, Z. Huang, S. Gaan, Recyclable inherently flame-retardant thermosets: Chemistry, properties and applications, Compos. B Eng. (2023), 110667, https://doi.org/10.1016/j.compositesb.2023.110667.

[33] W. Yang, H. Ding, W. Zhou, T. Liu, P. Xu, D. Puglia, J.M. Kenny, P. Ma, Design of inherent fire retarding and degradable bio-based epoxy vitrimer with excellent self-healing and mechanical reprocessability, Compos. Sci. Technol. (2022), 109776, https://doi.org/10.1016/j.compscitech.2022.109776.

[34] S. Majumdar, B. Mezari, H. Zhang, J. van Aart, R.A.T.M. van Benthem, J.P. A. Heuts, R.P. Sijbesma, Efficient Exchange in a Bioinspired Dynamic Covalent Polymer Network via a Cyclic Phosphate Triester Intermediate, Macromolecules 54 (17) (2021) 7955–7962, https://doi.org/10.1021/acs.macromol.1c01504.

[35] K.A. Salmeia, S. Gaan, An overview of some recent advances in DOPO-derivatives: Chemistry and flame retardant applications, Polym. Degrad. Stab. 113 (2015) 119–134, https://doi.org/10.1016/j.polymdegradstab.2014.12.014.

[36] X. Feng, G. Li, Catalyst-free β-hydroxy phosphate ester exchange for robust fire-proof vitrimers, Chem. Eng. J. 417 (2021), 129132, https://doi.org/10.1016/j.cej.2021.129132.

[37] G.P. Horsman, D.L. Zechel, Phosphonate Biochemistry, Chem. Rev. 117 (8) (2017) 5704–5783, https://doi.org/10.1021/acs.chemrev.6b00536.

[38] L.J. Schafer, K.J. Garcia, A.W. Baggett, T.M. Lord, P.M. Findeis, R.D. Pike, R. A. Stockland, Synthesis of Spirocyclic Diphosphite-Supported Gold Metallomacrocycles via a Protodeauration/Cyclization Strategy: Mechanistic and Binding Studies, Inorg. Chem. 57 (18) (2018) 11662–11672, https://doi.org/10.1021/acs.inorgchem.8b01805.

[39] T.M. Lord, S.L. Casino, S.E. Hartzell, K.J. Garcia, R.D. Pike, R.A. Stockland Jr, Convenient Access to Arylated Spirocyclic Bisphosphonates, ChemistrySelect 1 (10) (2016) 2188–2191, https://doi.org/10.1002/slct.201600479.

[40] R. Hardis, J.L.P. Jessop, F.E. Peters, M.R. Kessler, Cure kinetics characterization and monitoring of an epoxy resin using DSC, Raman spectroscopy, and DEA, Compos. A Appl. Sci. Manuf. 49 (2013) 100–108, https://doi.org/10.1016/j.compositesa.2013.01.021.

[41] R. Engel, Phosphonates as analogues of natural phosphates, Chem. Rev. 77 (3) (1977) 349–367, https://doi.org/10.1021/cr60307a003.

[42] P. Simonetti, R. Nazir, A. Gooneie, S. Lehner, M. Jovic, K.A. Salmeia, R. Hufenus, A. Rippl, J.-P. Kaiser, C. Hirsch, B. Rubi, S. Gaan, Michael addition in reactive extrusion: A facile sustainable route to developing phosphorus based flame retardant materials, Composites Part B-Engineering 178 (2019) 107470.

[43] S.T. Lazar, T.J. Kolibaba, J.C. Grunlan, Flame-retardant surface treatments, Nat. Rev. Mater. 5 (4) (2020) 259–275, https://doi.org/10.1038/s41578-019-0164-6.

[44] W. Cantwell, H. Kausch, Fracture behaviour of epoxy resins (1993) 144–174, https://doi.org/10.1007/978-94-011-2932-9_5.

[45] C.D. Varganici, L. Rosu, S. Lehner, C. Hamciuc, M. Jovic, D. Rosu, F. Mustata, S. Gaan, Semi–interpenetrating networks based on epoxy resin and oligophosphonate: Comparative effect of three hardeners on the thermal and fire properties, Mater. Des. 212 (2021), 110237, https://doi.org/10.1016/j.matdes.2021.110237.

[46] M. Podgórski, B.D. Fairbanks, B.E. Kirkpatrick, M. McBride, A. Martinez, A. Dobson, N.J. Bongiardina, C.N. Bowman, Toward Stimuli-Responsive Dynamic Thermosets through Continuous Development and Improvements in Covalent

Adaptable Networks (CANs), Adv. Mater. 32 (20) (2020) 1906876, https://doi.org/10.1002/adma.201906876.
[47] M. Hayashi, Versatile functionalization of polymeric soft materials by implanting various types of dynamic cross-links, Polym. J. 53 (7) (2021) 779–788, https://doi.org/10.1038/s41428-021-00474-2.
[48] W. Zou, J. Dong, Y. Luo, Q. Zhao, T. Xie, Dynamic Covalent Polymer Networks: from Old Chemistry to Modern Day Innovations, Adv. Mater. 29 (14) (2017) 1606100, https://doi.org/10.1002/adma.201606100.
[49] I.M. Kalogeras, Glass-Transition Phenomena in Polymer Blends (2016) 1–134, https://doi.org/10.1002/9783527653966.ch1.
[50] H. Fang, W. Ye, Y. Ding, H.H. Winter, Rheology of the Critical Transition State of an Epoxy Vitrimer, Macromolecules 53 (12) (2020) 4855–4862, https://doi.org/10.1021/acs.macromol.0c00843.
[51] Y. Shan, T. Liu, B. Zhao, C. Hao, S. Zhang, Y. Li, Y. Wu, J. Zhang, A renewable dynamic covalent network based on itaconic anhydride crosslinked polyglycerol: Adaptability, UV blocking and fluorescence, Chemical Engineering Journal 385 (2020), 123960, https://doi.org/10.1016/j.cej.2019.123960.
[52] B. Krishnakumar, R.V.S.P. Sanka, W.H. Binder, V. Parthasarthy, S. Rana, N. Karak, Vitrimers: Associative dynamic covalent adaptive networks in thermoset polymers, Chem. Eng. J. 385 (2020), 123820, https://doi.org/10.1016/j.cej.2019.123820.
[53] J.-H. Chen, B.-W. Liu, J.-H. Lu, P. Lu, Y.-L. Tang, L. Chen, Y.-Z. Wang, Catalyst-free dynamic transesterification towards a high-performance and fire-safe epoxy vitrimer and its carbon fiber composite, Green Chem. 24 (18) (2022) 6980–6988, https://doi.org/10.1039/D2GC01405J.
[54] X. Feng, J. Fan, A. Li, G. Li, Multireusable Thermoset with Anomalous Flame-Triggered Shape Memory Effect, ACS Appl. Mater. Interfaces 11 (17) (2019) 16075–16086, https://doi.org/10.1021/acsami.9b03092.
[55] A. Cohades, C. Branfoot, S. Rae, I. Bond, V. Michaud, Progress in Self-Healing Fiber-Reinforced Polymer Composites, Adv. Mater. Interfaces 5 (17) (2018) 1800177, https://doi.org/10.1002/admi.201800177.
[56] P. Zamani, O. Zabihi, M. Ahmadi, R. Mahmoodi, T. Kannangara, P. Joseph, M. Naebe, Biobased Carbon Fiber Composites with Enhanced Flame Retardancy: A Cradle-to-Cradle Approach, ACS Sustain. Chem. Eng. 10 (2) (2022) 1059–1069, https://doi.org/10.1021/acssuschemeng.1c07859.
[57] X. Liu, K.A. Salmeia, D. Rentsch, J.W. Hao, S. Gaan, Thermal decomposition and flammability of rigid PU foams containing some DOPO derivatives and other phosphorus compounds, J. Anal. Appl. Pyrol. 124 (2017) 219–229, https://doi.org/10.1016/j.jaap.2017.02.003.
[58] Y. Liu, B. Wang, S. Ma, X. Xu, J. Qiu, Q. Li, S. Wang, N. Lu, J. Ye, J. Zhu, Phosphate-based covalent adaptable networks with recyclability and flame retardancy from bioresources, Eur. Polym. J. 144 (2021), 110236, https://doi.org/10.1016/j.eurpolymj.2020.110236.
[59] J.-H. Chen, J.-H. Lu, X.-L. Pu, L. Chen, Y.-Z. Wang, Recyclable, malleable and intrinsically flame-retardant epoxy resin with catalytic transesterification, Chemosphere 294 (2022), 133778, https://doi.org/10.1016/j.chemosphere.2022.133778.
[60] S. Wang, S. Ma, Q. Li, W. Yuan, B. Wang, J. Zhu, Robust, Fire-Safe, Monomer-Recovery, Highly Malleable Thermosets from Renewable Bioresources, Macromolecules 51 (20) (2018) 8001–8012, https://doi.org/10.1021/acs.macromol.8b01601.
[61] S. Hörold, Phosphorus-based and Intumescent Flame Retardants, Polymer Green Flame Retardants (2014) 221–254, https://doi.org/10.1016/b978-0-444-53808-6.00006-8.
[62] S. Wendels, T. Chavez, M. Bonnet, K.A. Salmeia, S. Gaan, Recent Developments in Organophosphorus Flame Retardants Containing P-C Bond and Their Applications, Materials 10 (7) (2017), https://doi.org/10.3390/ma10070784.
[63] A. Bifulco, D. Parida, K.A. Salmeia, S. Lehner, R. Stämpfli, H. Markus, G. Malucelli, F. Branda, S. Gaan, Improving flame retardancy of in-situ silica-epoxy nanocomposites cured with aliphatic hardener: Combined effect of DOPO-based flame-retardant and melamine, Composites Part C: Open Access 2 (2020), 100022, https://doi.org/10.1016/j.jcomc.2020.100022.